Published in final edited form as:

ChemPhotoChem. 2021 May ; 5(5): 421–425. doi:10.1002/cptc.202000283.

It Takes Three to Tango – the length of the oligothiophene determines the nature of the long-lived excited state and the resulting photocytotoxicity of a Ru(II) photodrug

Avinash Chettri[a,b], **John A. Roque III**[c,d], **Kilian R. A. Schneider**[a,b], **Houston D. Cole**[c], **Colin G. Cameron**[c], **Sherri A. McFarland**[c,*], **Benjamin Dietzek**[a,b,*]

[a]Department Functional Interfaces Department, Leibniz Institute of Photonic Technology Jena, Albert-Einstein-Straße 9, 07745 Jena, Germany

[b]Institute of Physical Chemistry, Friedrich-Schiller University Jena, Helmholtzweg 4, 07743 Jena, Germany

[c]Department of Chemistry and Biochemistry, The University of Texas Arlington, Arlington, TX 76019, USA

[d]Department of Chemistry and Biochemistry, The University of North Carolina at Greensboro, Greensboro, North Carolina 27402, USA

Abstract

TLD1433 is the first Ru(II) complex to be tested as a photodynamic therapy agent in a clinical trial. In this contribution we study TLD1433 in the context of structurally-related Ru(II)-imidozo[4,5-f][1,10]phenanthroline (ip) complexes appended with thiophene rings to decipher the unique photophysical properties which are associated with increasing oligothiophene chain length. Substitution of the ip ligand with ter- or quaterthiophene changes the nature of the long-lived triplet state from metal-to-ligand charge-transfer to $^3\pi\pi^*$ character. The addition of the third thiophene thus presents a critical juncture which not only determines the photophysics of the complex but most importantly its capacity for $^1O_2$ generation and hence the potential of the complex to be used as a photocytotoxic agent.

Entry for the Table of Contents—A low-lying triplet intraligand state (^{3}IL) determines the properties of the long-lived excited states in a series of Ru(II) complexes. The ^{3}IL state can be accessed by increasing the length of an oligothiophene chain. The ^{3}IL state is extremely efficient at generating $^1O_2$ and thus enhances the potency of the complexes as PDT agents.

*corresponding authors: Benjamin.dietzek@leibniz-ipht.de; sherri.mcfarland@uta.edu.

Conflict of interest

S. A. M. has a potential research conflict of interest due to a financial interest with Theralase Technologies, Inc. and PhotoDynamic, Inc. A management plan has been created to preserve objectivity in research in accordance with UTA policy.

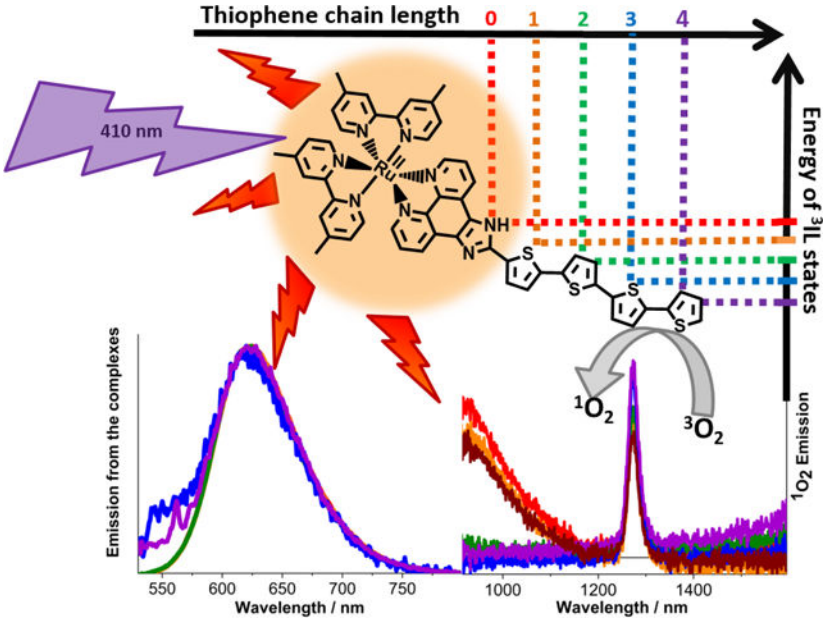

Keywords

TLD1433; PDT; long-lived triplet states; singlet oxygen; lifetimes

Introduction

Recent developments highlight Ru(II) polypyridyl complexes with π-expanded ligands as a promising class of new compounds for photodynamic therapy (PDT).[1–11] By extending the pyridyl ligands with organic chromophores, low-lying intraligand (IL) excited states become accessible, and these appear to be crucial to the photophysical function of these systems.[12] Our TLD1433 (**Ru-ip-3T** in this manuscript, Figure 1) is a compound of this type, having three appended thiophene rings, and has the distinction of being the first Ru(II)-based PDT agent ever to enter a human clinical trial;[1,10,13] **Ru-ip-3T** is currently being tested in a Phase II PDT trial for non-invasive bladder cancer (ClinicalTrials.gov identifier: NCT03945162).[10]

In vitro studies have been previously conducted on the **Ru-ip-*n*T** series of compounds, where *n* indicates the number of appended thiophene rings attached to an imidazo[4,5-*f*][1,10]phenanthroline (ip) ligand (Figure 1). Visible light illumination of SK-MEL-28 cancer cells treated with the compounds in the series led to increased photocytotoxicity with increasing *n*. The EC_{50} values (effective concentration to reduce cell viability by 50%) were 0.72 μM, 0.26 μM, 1.9×10^{-4} μM and 2.8×10^{-9} μM for **Ru-ip-1T** to **Ru-ip-4T**, respectively (Figure 2d).[1] While these previous findings demonstrate a clear correlation between the length of the thiophene chain and the in vitro phototherapeutic effects, herein we present the key photophysical properties of the compounds in the **Ru-ip-*n*T** series that could be responsible for the observed photocytotoxicity.

Results and Discussion

STEADY STATE ABSORPTION AND EMISSION SPECTROSCOPY

The electronic absorption spectra of the compounds within the **Ru-ip-*n*T** series (Figure 2a) are characterized by IL transitions localized to the dmb and phen portion of the ip ligand below 300 nm as well as a broad metal-to-ligand charge transfer (MLCT) band in the 420–550 nm range, consistent with the spectrum of the parent $[Ru(dmb)_3]^{2+}$ complex.[14,15] An additional band centered near 370 nm is visible in **Ru-ip-2T** that shifts to longer wavelengths in **Ru-ip-3T** and **Ru-ip-4T**. This band corresponds to the $\pi\pi^*$ ^{1}IL transition associated with the oligothiophene.[16] These oligothiophene-localized transitions have been computed to have substantial charge transfer character and are best described as intraligand charge transfer (ILCT) states, but are referred to herein more generally as IL.[17,18]

The steady-state emission spectra of the complexes show a single structureless emission band centered at 625 nm (Figure 2b), suggesting a similar emissive ^{3}MLCT state for all complexes in the **Ru-ip-*n*T** family.[19] The emission quantum yields ($\Phi_{em.}$) in deaerated water (five freeze pump thaw cycles under a nitrogen atmosphere) drop with increasing *n*, from 6% for **Ru-ip-1T** to below 0.1% for **Ru-ip-3T** (Table 1). Emission from **Ru-ip-4T** is barely detectable (Figure 2d). The emission quantum yields for **Ru-ip-3T** and **Ru-ip-4T** are extremely small and do not notably increase upon deaeration of the solvent. This suggests that collisional deactivation by $^3O_2$ is not the prime quenching process of the ^{3}MLCT state in the complexes.

The excitation spectra recorded for **Ru-ip-0T**, **Ru-ip-1T** and **Ru-ip-2T** using the emission signal at 640 nm resemble the respective absorption spectra (Figure 2a, b), suggesting that the emissive ^{3}MLCT state is populated regardless of whether the initially populated states are ^{1}MLCT or ^{1}IL (i.e., $\pi\pi^*$). The absence of excitation signals that would correspond to broad ^{1}IL transitions in the UV-vis spectra at 420 nm and 440 nm for **Ru-ip-3T** and **Ru-ip-4T**, respectively, indicates that excitation of the ^{1}IL state does not populate the emissive ^{3}MLCT state.

In addition to absorption and emission characteristics, the singlet oxygen quantum yields (Φ_Δ) were also measured. Values for Φ_Δ increase from 0.61 for **Ru-ip-1T** to 0.81 for **Ru-ip-4T** (Table 1). This trend is consistent with the trend for photocytotoxicity as reflected in the PI values that increase with *n* (see Figure 2d). This positive correlation between singlet oxygen quantum yields and photocytotoxicity suggests that singlet oxygen is involved in their mode of action.[20–22] Enhanced sensitivity toward oxygen is normally reflected as a drastic decrease in triplet excited state lifetime in the presence of oxygen.[8] The relative changes of excited state lifetimes for **Ru-ip-*n*T** upon exposure to oxygen will be discussed in the next section.

TRANSIENT ABSORPTION AND EMISSION LIFETIMES

The photophysical properties of the longer-lived excited states, from which singlet oxygen sensitization occurs, were probed by transient absorption (TA) spectroscopy yielding excited-state absorption spectra and characteristic time-constants for ground state recovery

(τ_{TA}) and emission decay (τ_{em}). Table 1 summarizes these key characteristics of the long-lived excited states in aerated or deaerated water. The emission and TA lifetimes of **Ru-ip-0T** and **Ru-ip-1T** are the same, 0.4 μs, indicative of a single excited state being depopulated (Figure 3a). The fact that deaeration lengthens the lifetime by only two-fold suggests that this state is only weakly quenched by oxygen. **Ru-ip-2T** behaves somewhat differently than **Ru-ip-0T** and **Ru-ip-1T**. In aerated aqueous solutions, τ_{em} and τ_{TA} for **Ru-ip-2T** are 1 μs and 1.4 μs, respectively. In deaerated solutions, however, the excited state(s) was much longer lived, and the emission decay was biexponential (τ_{em}=0.6; 11 μs, τ_{TA}=14 μs). An excited state lifetime that is ten-fold (or more) longer than the typical 1 μs lifetime of ^{3}MLCT states in Ru(II) polypyridyl complexes and is very sensitive to O_2 is consistent with the involvement of an ^{3}IL state.[23,24] The second thiophene lowers the energy of this state sufficiently that the emissive ^{3}MLCT and non-emissive ^{3}IL states are in energetic proximity (Figure 3b). The biexponential emission decay, where the longer component matches the decay of the nonemissive state by TA, suggests that the shorter 0.6-μs component is due to prompt ^{3}MLCT emission and the longer 11-μs lifetime corresponds to delayed emission from the ^{3}MLCT state resulting from population of the ^{3}MLCT from the nearly isoenergetic ^{3}IL state (Figure 3b).[24]

For **Ru-ip-3T** and **Ru-ip-4T**, the aerated and deaerated emission lifetimes were monoexponential and relatively short ($\tau_{em}\approx$0.4 μs) as observed for **Ru-ip-0T** and **Ru-ip-1T**, indicating that the emissive ^{3}MLCT state cannot be populated from the ^{3}IL when n=3 or 4. **Ru-ip-3T** and **Ru-ip-4T** are barely emissive, with emission quantum yields too small to be calculated in the aerated solutions and vanishingly small in deaerated conditions. These observations point to the fact that a significant fraction of the **Ru-ip-3T** and **Ru-ip-4T** excited states must deactivate via non-emissive ^{3}IL states. The aerated TA lifetimes for **Ru-ip-3T** and **Ru-ip-4T** were identical to that of **Ru-ip-2T**, consistent with efficient quenching of the ^{3}IL states by O_2 and corroborated by all three being very good $^1O_2$ sensitizers. The values for τ_{TA} in deaerated water were considerably longer, 48 μs and 29 μs for **Ru-ip-3T** and **Ru-ip-4T**, respectively. This is attributed to the ^{3}IL state of both **Ru-ip-3T** and **Ru-ip-4T** being sufficiently lower in energy than the emissive ^{3}MLCT state (Figure 3c), which remains unchanged throughout the series (evidenced by a constant emission maximum). The triplet is thereby trapped in the longer-lived ^{3}IL state, unable to populate the ^{3}MLCT, which is significantly uphill in energy. The ^{3}IL relaxes much slower due to the reduced intersystem crossing rate in organic chromophores compared to transition metal complexes, in which the heavy metal ion increases spin-orbit coupling. The lifetime of the ^{3}IL state for **Ru-ip-4T** may be shorter than the corresponding lifetime for **Ru-ip-3T** due to the energy gap law.[25] However, additional relaxation pathways cannot be excluded without further investigation.

The change in the nature of the long-lived photobiologically active excited states is also supported by the spectral shape of the ns TA spectra within the **Ru-ip-*n*T** series. The TA spectra of **Ru-ip-0T** and **Ru-ip-1T** show a ground-state bleach below 510 nm plus a very weak, unstructured excited-state absorption extending from 510 to 800 nm (Figure 2c). This signature is typical for the ^{3}MLCT states of Ru(II) polypyridyl complexes that lack π-extended ligands and thus low-lying ^{3}IL states.[26] The TA spectra change substantially for **Ru-ip-2T** through **Ru-ip-4T**, which have very strong and much more structured excited

state absorptions with maxima at 550, 630, and 680 nm, respectively. This systematic red-shift of the excited state absorption with increasing *n*, by over 100 nm, is characteristic of oligothiophene-based ^{3}IL states.[5,17] Thus, the ns TA spectra indicate that the character of the long-lived state changes from ^{3}MLCT for **Ru-ip-0T** and **Ru-ip-1T** to predominantly ^{3}IL with additional thiophene rings.

Conclusion

This study highlights the photophysical properties of the long-lived excited states in a series of Ru(II) complexes, which underlie their previously reported photocytotoxicity. The results show that the spectroscopic signatures of the long-lived excited states and the biological activity in this series of complexes are determined by the energy of the non-emissive ^{3}IL state relative to the energy of the emissive ^{3}MLCT state. This energy depends on the length of the oligothiophene chain and determines the TA absorption and emission lifetimes, emission quantum yields and light EC_{50} values. In **Ru-ip-0T** and **Ru-ip-1T** the energy of the ^{3}IL is too high and the state does not contribute to the ns-/μs-photophysics and photobiology of the complexes. **Ru-ip-2T** represents the situation where the ^{3}MLCT and ^{3}IL states are close in energy. In this case, the ^{3}IL state serves as an excited state reservoir for populating the ^{3}MLCT state and results in delayed ^{3}MLCT emission. In **Ru-ip-3T** and **Ru-ip-4T** the ^{3}IL state is the lowest-lying triplet and plays a predominant role in the excited state relaxation. The oxygen-sensitive ^{3}IL state appears to be responsible for the increased photocytotoxicity of these complexes. This is manifested in a sharp increase in the photocytotoxicity and efficiency of singlet oxygen sensitization upon increasing the length of the oligothiophene chain.

Experimental Section

All samples were dissolved in the respective solvent and measured in a 1 cm quartz cell. All solvents were deaerated by freeze pump thaw cycles for five times using nitrogen as inert gas. For measuring $\Phi_{em.}$ and Φ_Δ samples with an OD of about 0.05 were used. Quantum yields were calculated according to the the equation $\Phi_s = \Phi_r \cdot \frac{I_s}{I_r} \cdot \frac{OD_r}{OD_s} \cdot \frac{\eta_r^2}{\eta_s^2}$ where Φ_s and Φ_r are the quantum yields of the sample and a reference, respecitively. I_s and I_r are the integrated emission intensity of the sample and the references, while OD_r and OD_s are the optical densities of the sample and the reference at the excitation wavelength. η_r and η_s refer to the refractive indices of the media in the sample and the reference. Since the same medium is used for measuring the sample and the reference $\frac{\eta_r^2}{\eta_s^2}$ equals 1.

UV-vis absorption measurements utilized a Jasco V-670 spectrophotometer and emission measurements were carried out on a FLS980 spectrophotometer (Edinburgh Instruments). $^1O_2$ emission was detected using a FLS980 spectrophotometer equipped with a NIR detector with parameters upon excitation at 450 nm.

Nanosecond transient absorption measurements used a 10 Hz Nd:YAG laser (Surelite) combined with an OPO for excitation. The Transient data was recorded by a commercial

detection system (Pascher Instruments AB) with a time resolution of 10 ns. The OD of the samples at the excitation wavelength was ~0.25 in a 1-cm cuvette. The integrity of the samples after nanosecond measurements were checked by measuring absorption spectra before and after the measurement. No degradation was observed. Time resolved emission measurements utilized time correlation single photon counting (TCSPC, Becker & Hickl GmbH) upon excitation at 390 nm.

Acknowledgements

We are grateful to the German Science Foundation (grant No. 395358570), the Carl Zeiss Foundation. We also thank the National Cancer Institute (NCI) of the National Institutes of Health (NIH) (Award R01CA222227) for partial support of this work. The content in this article is solely the responsibility of the authors and does not necessarily represent the official views of the National Institutes of Health.

References

[1]. Monro S, Colón KL, Yin H, Roque J, Konda P, Gujar S, Thummel RP, Lilge L, Cameron CG, McFarland SA, Chem. Rev 2019, 119, 797–828. [PubMed: 30295467]

[2]. Stephenson M, Reichardt C, Pinto M, Wa M, Sainuddin T, Shi G, Yin H, Monro S, Sampson E, Dietzek B, Mcfarland SA, J. Phys. Chem. A 2014, 10507–10521.

[3]. Chakrabortty S, Agrawalla BK, Stumper A, Vegi NM, Fischer S, Reichardt C, Kögler M, Dietzek B, Feuring-Buske M, Buske C, Rau S, Weil T, J. Am. Chem. Soc 2017, 139, 2512–2519. [PubMed: 28097863]

[4]. Howerton BS, Heidary DK, Glazer EC, J. Am. Chem. Soc 2012, 134, 8324–8327. [PubMed: 22553960]

[5]. Ghosh G, Colón KL, Fuller A, Sainuddin T, Bradner E, McCain J, Monro SMA, Yin H, Hetu MW, Cameron CG, McFarland SA, Inorg. Chem 2018, 57, 7694–7712. [PubMed: 29927243]

[6]. Sainuddin T, McCain J, Pinto M, Yin H, Gibson J, Hetu M, McFarland SA, Inorg. Chem 2016, 55, 83–95. [PubMed: 26672769]

[7]. Sainuddin T, Pinto M, Yin H, Hetu M, Colpitts J, McFarland SA, J. Inorg. Biochem 2016, 158, 45–54. [PubMed: 26794708]

[8]. Lincoln R, Kohler L, Monro S, Yin H, Stephenson M, Zong R, Chouai A, Dorsey C, Hennigar R, Thummel RP, McFarland SA, J. Am. Chem. Soc 2013, 135, 17161–17175.

[9]. Reichardt C, Pinto M, Wächtler M, Stephenson M, Kupfer S, Sainuddin T, Guthmuller J, McFarland SA, Dietzek B, J. Phys. Chem. A 2015, 119, 3986–3994. [PubMed: 25826128]

[10]. Shi G, Monro S, Hennigar R, Colpitts J, Fong J, Kasimova K, Yin H, DeCoste R, Spencer C, Chamberlain L, Mandel A, Lilge L, McFarland SA, Coord. Chem. Rev 2015, 282–283, 127–138.

[11]. Yin H, Stephenson M, Gibson J, Sampson E, Shi G, Sainuddin T, Monro S, McFarland SA, Inorg. Chem 2014, 53, 4548–4559. [PubMed: 24725142]

[12]. Albani BA, Peña B, Leed NA, De Paula NABG, Pavani C, Baptista MS, Dunbar KR, Turro C, J. Am. Chem. Soc 2014, 136, 17095–17101.

[13]. McFarland SA, Mandel A, Dumoulin-White R, Gasser G, Curr. Opin. Chem. Biol 2020, 56, 23–27.

[14]. Tamaki Y, Tokuda K, Yamazaki Y, Saito D, Ueda Y, Ishitani O, Front. Chem 2019, 7, 1–9. [PubMed: 30778383]

[15]. Damrauer NH, McCusker JK, J. Phys. Chem. A 1999, 103, 8440–8446.

[16]. Grebner D, Helbig M, Rentsch S, J. Phys. Chem 1995, 99, 16991–16998.

[17]. Roque JA III, Barrett PC, Cole HD, Lifshits LM, Bradner E, Shi G, von Dohlen D, Kim S, Russo N, Deep G, Cameron CG, Alberto ME, McFarland SA, Inorg. Chem 2020, 59, 16341–16360.

[18]. Roque JA III, Barrett PC, Cole HD, Lifshits LM, Shi G, Monro S, Von Dohlen D, Kim S, Russo N, Deep G, Cameron CG, Alberto ME, McFarland SA, Chem. Sci 2020, 11, 9784–9806. [PubMed: 33738085]

[19]. Curtright AE, McCusker JK, J. Phys. Chem. A 1999, 103, 7032–7041.

[20]. Lifshits LM, Roque III JA, Konda P, Monro S, Cole HD, von Dohlen D, Kim S, Deep G, Thummel RP, Cameron CG, Gujar S, McFarland SA, Chem. Sci 2020, 11740–11762.

[21]. Reichardt C, Monro S, Sobotta FH, Colón KL, Sainuddin T, Stephenson M, Sampson E, Roque J, Yin H, Brendel JC, Cameron CG, McFarland S, Dietzek B, Inorg. Chem 2019, 58, 3156–3166. [PubMed: 30763081]

[22]. MacDonald IJ, Dougherty TJ, J. Porphyr. Phthalocyanines 2001, 5, 105–129.

[23]. Wang XY, Del Guerzo A, Schmehl RH, J. Photochem. Photobiol. C Photochem. Rev 2004, 5, 55–77.

[24]. McClenaghan ND, Leydet Y, Maubert B, Indelli MT, Campagna S, Coord. Chem. Rev 2005, 249, 1336–1350.

[25]. Englman R, Jortner J, Mol. Phys 1970, 18, 285–287.

[26]. Peuntinger K, Pilz TD, Staehle R, Schaub M, Kaufhold S, Petermann L, Wunderlin M, Görls H, Heinemann FW, Li J, Drewello T, Vos JG, Guldi DM, Rau S, Dalt. Trans 2014, 43, 13683–13695.

[27]. Suzuki K, Kobayashi A, Kaneko S, Takehira K, Yoshihara T, Ishida H, Shiina Y, Oishi S, Tobita S, Phys. Chem. Chem. Phys 2009, 11, 9850–9860. [PubMed: 19851565]

[28]. Abdel-Shafi AA, Beer PD, Mortimer RJ, Wilkinson F, Helv. Chim. Acta 2001, 84, 2784–2795.

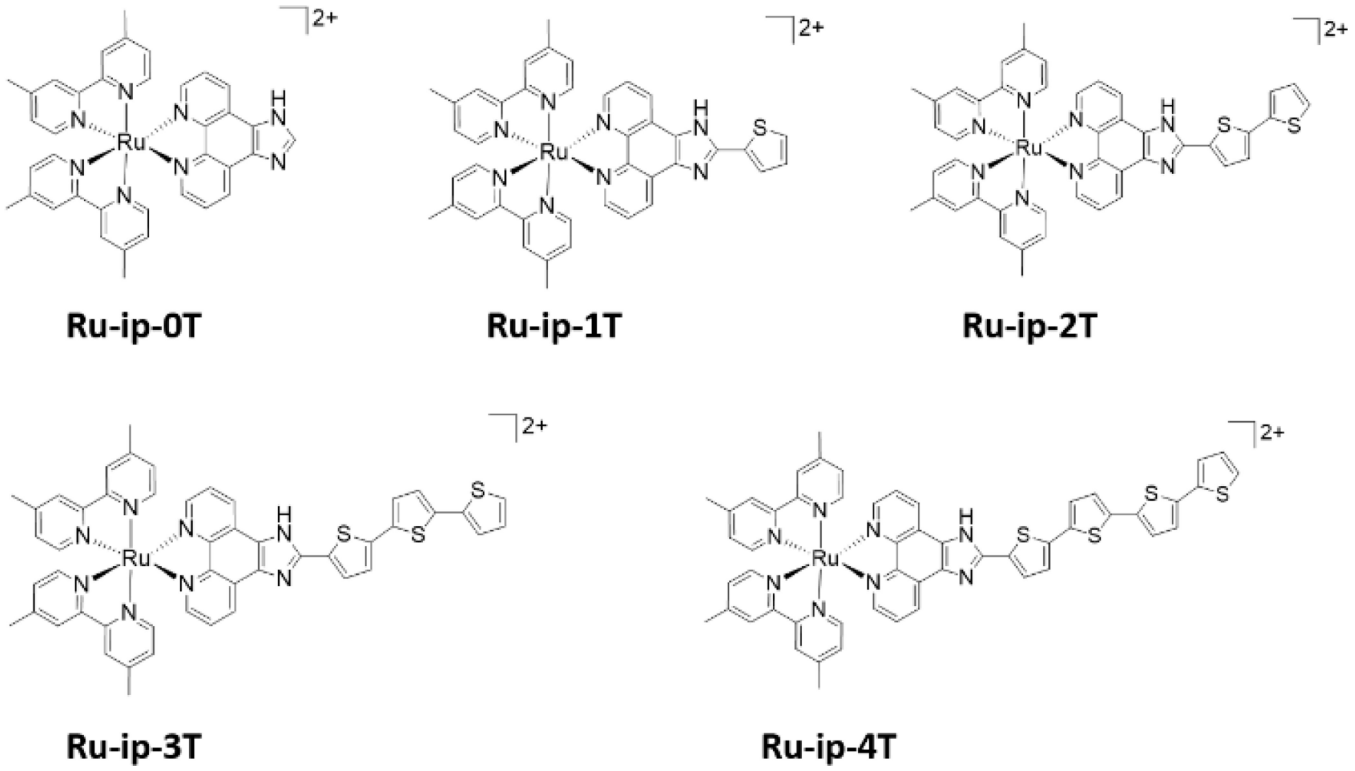

Figure 1.
Chemical structures of **Ru-ip-*n*T** complexes.

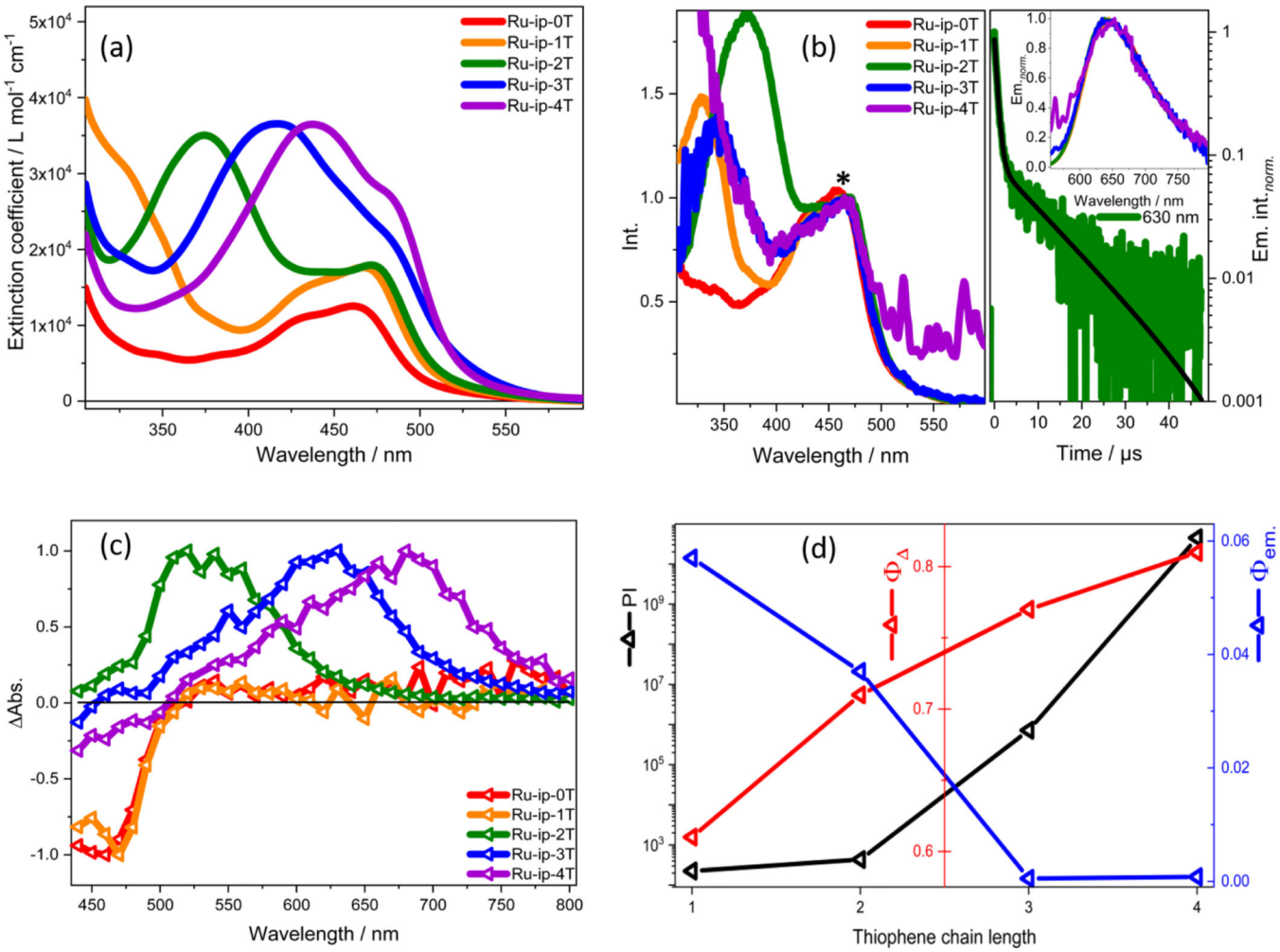

Figure 2.

(a) Absorption spectra for the **Ru-ip-*n*T** complexes in water. (b) Excitation spectra of the **Ru-ip-*n*T** complexes in water at 640 nm emission normalized to the MLCT band at 480 nm (*, left); bi-exponential emission decay of **Ru-ip-2T** with lifetimes of 0.6 μs and 11 μs at 630 nm (right); Inset: Emission spectra of **Ru-ip-*n*T** complexes normalized to their respective maxima. (c) Nanosecond TA spectra of **Ru-ip-*n*T** complexes in aerated water normalized to their respective maxima at $\lambda_{ex.}$: 410 nm at 300 ns. (d) Relationship between the PI values (black y-axis), singlet-oxygen quantum yield Φ_{Δ} (red y-axis) in aerated MeCN (excitation at 450 nm) and fluorescence quantum yield $\Phi_{em.}$ (blue y-axis) in deaerated water (excitation at 450 nm) with increasing thiophene chain length (x-axis).[1] The PI is defined as the ratio of $EC_{50\ dark}$ to $EC_{50\ visible\ light}$ values in SK-MEL-28 cells.

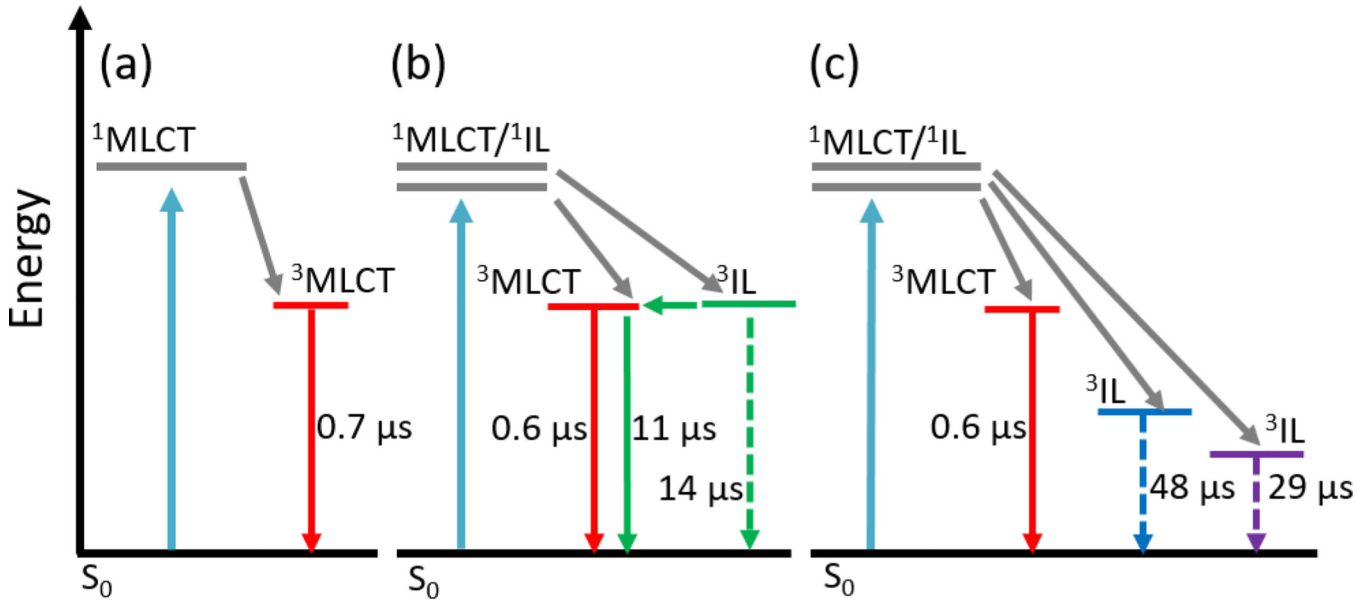

Figure 3.

Jablonski diagrams depicting the photophysical models that describe the nanosecond-microsecond excited state dynamics of **Ru-ip-*n*T** complexes with 410 nm excitation in deaerated water: (a) **Ru-ip-0T**, **Ru-ip-1T;** (b) **Ru-ip-2T**; (c) **Ru-ip-3T, Ru-ip-4T.** [Note: grey arrows represent processes occurring faster than the investigated timescale.]

Table 1.

Excited state lifetimes and quantum yields for emission and singlet oxygen production for **Ru-ip-nT**under different conditions.

Complex	$\tau_{em.}$ [c]		$\tau_{TA.}$ [c]		$\Phi_{em.}$ [c]		Φ_{Δ} [d]
	Aerated (μs)	Deaerated (μs)	Aerated (μs)	Deaerated (μs)	Aerated	Deaerated	
Ru-ip-0T	0.4	0.7	0.4	0.7	0.038	0.05	0.68
Ru-ip-1T	0.4	0.8	0.4	0.7	0.044	0.06	0.61
Ru-ip-2T	0.3; 1 [a]	0.6; 11 [a]	1.4	14	0.006	0.04	0.71
Ru-ip-3T	0.3	0.6	1.4	48	- [b]	4.8×10^{-4}	0.77
Ru-ip-4T	0.3	0.6	1.4	29	- [b]	8.1×10^{-4}	0.81

$\tau_{em.}$: emission lifetime; $\tau_{TA.}$: recovery lifetime; $\Phi_{em.}$: quantum yield of emission; Φ_{Δ}: singlet oxygen quantum yield. Singlet oxygen was determined spectroscopically by monitoring its emission centered at 1275 nm in aerated MeCN. **$[Ru(bpy)_3][PF_6]_2$** is used as the reference obtaining $\Phi_{em.}$[27] and Φ_{Δ}.[28]

[a] A biexponential decay of the respective signal is observed.

[b] Emission is too low to obtain a reasonable estimate of the emission quantum yield.

[c] Solvent used is H_2O.

[d] Solvent used is MeCN.